Two-color photons and nonlocality in fourth-order interference

J. G. Rarity and P. R. Tapster
Royal Signals and Radar Establishment, Saint Andrews Road, Malvern, Worcester WR14 3PS, United Kingdom
(Received 11 December 1989)

Angle-separated pair photons emitted in spontaneous parametric fluorescence are superimposed at a beamsplitter and detected by coincidence techniques. The coincidence disappears when the photon path lengths to the beamsplitter are equal to within their inverse bandwidth due to fourth-order interference. The photon bandwidth is set by wide apertures placed to satisfy phase-matching conditions at the nonlinear crystal. The resulting broadband photons are short (39-fs full width at half maximum) and show an oscillatory tail resulting from the hard-edge apertures. Two-color photons are created by blocking the central portion of the apertures leading to strong oscillations of the coincidence rate as a function of path-length difference. Both effects are predicted by the theory of fourth-order interference coupled with the detailed phase-matching conditions in the nonlinear crystal used as a source. The two colors overlap at different positions on the beamsplitter. We show how this could be used as a test of local realistic theories by formulating a Bell inequality based on relative phases between the colors.

I. INTRODUCTION

A $|1,1\rangle$ photon state can be selected in nondegenerate parametric downconversion experiments by photon-counting coincidence detection.[1,2] The disappearance of this coincidence after recombination at a beamsplitter has recently been studied theoretically[3–7] and experimentally.[8–10] The range of path-length differences over which the effect can be seen is related by Fourier transform to the pair-photon bandwidth. In nondegenerate parametric downconversion the bandwidth of the pair photons can be set by apertures placed to satisfy the phase- (and energy-) matching conditions at the nonlinear crystal. In principle aperture size is not limited to a single mode of the downconverted field. In this series of experiments we have used wide horizontal slits as apertures and develop a thin-crystal theory relating the shape of the coincidence reduction as a function of path-length difference to the Fourier transform of the aperture (Sec. II). Extension of the theory to encompass thick crystals is discussed in the Appendix. A pair-photon width of 39 fs [11.7-μm full width at half maximum (FWHM)] is measured for apertures subtending an angle of 14.5 mrad at the nonlinear crystal. This effect is much shorter than previously measured[8,9] and in principle only limited by aperture size for thin crystals. Furthermore, due to the use of larger multimode apertures and efficient near-infrared detectors the coincidence rates measured in this experiment are 3 orders of magnitude higher than the initial measurements of this type,[8] allowing one to propose practical uses for these nonclassical effects.

The wavelength of the downconverted light changes across the extent of the slit aperture due to the phase-matching condition at the crystal. We create spatially separated two-color photons by blocking the centers of the apertures. The coincidence rate then shows a cosinusoidal oscillation within a Gaussian envelope as the path-length difference is scanned through zero delay. This effect is predicted by a simple two-point aperture theory. A similar fourth-order spatial beating effect has previously been seen with nonmatched interference filters in front of the coincidence detectors.[10] In our experiment, however, the colors are spatially separated demonstrating that the effects are not only nonclassical but also nonlocal. In principle violations of local realism can be demonstrated. We discuss (Sec. IV) a rearrangement of the apparatus which could be used to test Bell's inequality without use of polarizers.

II. THEORY

We consider a general source of angle-separated correlated photon pairs (see Fig. 1) in the low-flux limit when the number of photons per mode is very much less than one. Photon pairs are detected using two suitably placed photon-counting detectors coupled to a coincidence counter with variable delay circuitry. The chance of random photon overlap within a short coincidence gate time ΔT set by the coincidence counter can be made small compared to the probability of photon pair detections at zero delay. The coincidence rate $\bar{C}_{12}$ for detection of photon pairs in directions 1 and 2 can thus be measured by subtraction of the random background (either calculated or measured at nonzero delay) from the zero-delay coincidence peak. This coincidence rate has been shown to be proportional to the square modulus of the pair-photon probability amplitude $g_{12}(\Delta t)$ (Ref. 2) integrated over the coincidence gate width

$$\bar{C}_{12}=\beta\int_{-\Delta T/2}^{+\Delta T/2}|g_{12}(\Delta t+\tau)|^2 d\tau \tag{1}$$

with β a constant of proportionality and

$$g_{12}(\Delta t)\equiv\langle \hat{A}_1^{(+)}(t_1,\mathbf{X}_1)\hat{A}_2^{(+)}(t_2,\mathbf{X}_2)\rangle \tag{2}$$

where $\hat{A}^{(+)}(t,\mathbf{X})$ is the positive frequency part of the electric field operator at time t and position $\mathbf{X}$ with

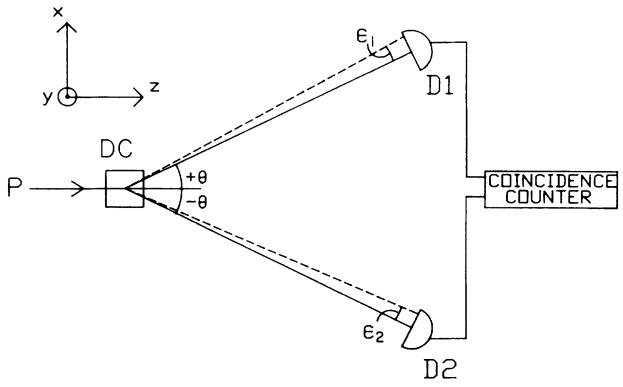

FIG. 1. Schematic diagram of an angle correlated pair-photon source. Photon-counting detectors D1 and D2 view a parametric downconversion crystal DC illuminated by a short-wavelength pump beam P. The standardized photoelectron pulses produced are sent to a multidelay coincidence counter for analysis. The symmetric phase-matching angles $\pm\theta$, and difference angles ϵ_1,ϵ_2 are also shown along with the axis convention used throughout this paper.

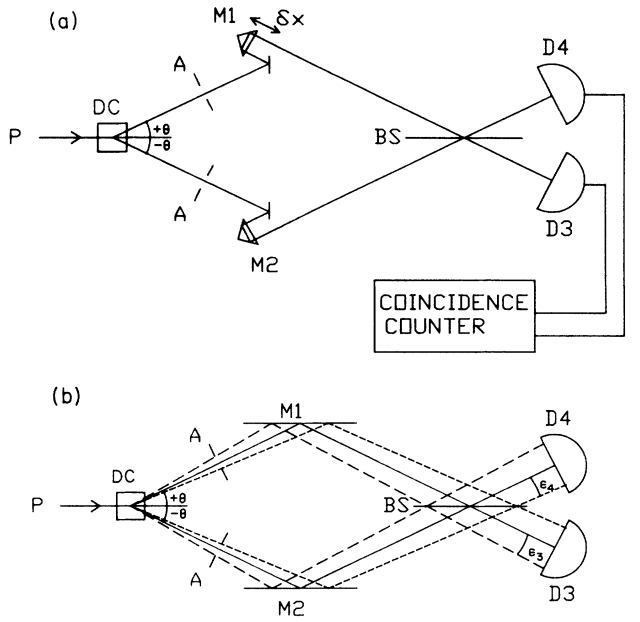

FIG. 2. (a) Block diagram of the fourth-order interference apparatus. Apertures A are used to limit the pair-photon bandwidth. Mirror assembly M2 is fixed while M1 is used to adjust the path-length difference δx to the beamsplitter BS. Detectors are now labeled D3, D4 to emphasize that they see light from paths 1 and 2 through the beamsplitter. (b) The geometry relating to the calculation of the fourth-order interference effect when extended apertures are used. The difference angles ϵ_3,ϵ_4 measured at the detectors are projected back through the beamsplitter adding to $\pm\theta$ in transmission while they are subtracted in reflection.

respect to the source. The subscripts refer to detectors (and direction) and the reduced time difference

$$\Delta t=\bar{t}_1-\bar{t}_2,\quad \bar{t}_{1,2}=t_{1,2}-X_{1,2}/c\ . \tag{3}$$

If, instead of detecting the photons emitted in directions 1 and 2, we superpose them at a beamsplitter (see Fig. 2) and detect them in detectors D3 and D4 placed to view the beamsplitter outputs, the coincidence rate $\bar{C}$(D3,D4) can be calculated from[8,9]

$$\bar{C}(\mathrm{D3,D4})\propto R^2\bar{C}_{3'4'}+T^2\bar{C}_{34}-\beta RT\left[\int_{-\infty}^{\infty} g^*_{3'4'}(\Delta t-\tau)\times g_{43}(\Delta t+\tau)d\tau+\mathrm{c.c.}\right] \tag{4}$$

where R and T are the intensity reflection and transmission coefficients of the beamsplitter and we have assumed that the electronically set coincidence gate width ΔT is much greater than any path-length-induced delay between photodetections or pair-photon coincidence uncertainty allowing the approximation $\Delta T\sim\infty$. The directions 3 and 4 correspond to fields transmitted through the beamsplitter while 3′ and 4′ correspond to reflected fields. It is this fourth-order mixing of two reflected and two transmitted fields evident in the third term of Eq. (4) which leads to the counter-intuitive fourth-order interference effects.

In this work the pair-photon source is a (second-order) nonlinear birefringent crystal illuminated by a strong short-wavelength pump beam (wave vector $\mathbf{k}_0$ and angular frequency ω_0). The crystal is cut so that the phase-matching conditions favor nondegenerate parametric downconversion (spontaneous parametric fluorescence). The pair-photon probability amplitude in directions 1 and 2 can be obtained from a coherent summation over the illuminated region within the crystal of all the conjugate frequencies contributing to the two-photon wave packet.[2] We write

$$g_{12}\propto\int\int d\omega_1 d\omega_2\omega_1\omega_2\chi^{(2)}(\omega_0,\omega_1,\omega_2)\delta(\omega_0-\omega_1-\omega_2)\times e^{-i(\omega_1\bar{t}_1+\omega_2\bar{t}_2)}\times\int d^3r e^{i(\mathbf{k}_1+\mathbf{k}_2-\mathbf{k}_0)\cdot\mathbf{r}}h(\mathbf{r}) \tag{5}$$

where $\chi^{(2)}$ is the relevant component of the second-order nonlinear optic tensor, $h(\mathbf{r})$ defines the illuminated region within the nonlinear crystal as a function of position $\mathbf{r}$ measured from the center of the crystal, and the convention of an incident plane-wave beam traveling in the z direction is assumed. Downconverted light in direction 1,2 has wave vector $\mathbf{k}_{1,2}$ (inside the crystal), angular frequency $\omega_{1,2}$, and energy conservation ($\omega_1+\omega_2\equiv\omega_0$) is implicit in the δ function. For large illuminated volumes the phase-matching integral reduces to the simplistic phase-matching condition $\mathbf{k}_0=\mathbf{k}_1+\mathbf{k}_2$. For this phase-matching condition to be satisfied the short-wavelength refractive index must be less than that for longer wavelengths. This can be achieved in a birefringent crystal when one or both downconverted photons are polarized orthogonal to the pump-beam polarization. In this work

we assume type-1 phase matching where both downconverted photons are polarized orthogonal to the incident pump beam and see similar refractive indices n within the crystal. We also make a narrowband approximation (valid to 10% relative bandwidth) by assuming $\omega_1\omega_2\chi^{(2)}(\omega_0,\omega_1,\omega_2)$ to be constant in the following.

For apertures placed a finite distance from a large illuminated volume the wave vectors themselves become dependent on position $\mathbf{r}$. In this work we assume far-field apertures hence ignore any position dependence of wave vectors. For small angles between directions 1,2 and the z axis (pump-beam direction) the wave vectors within the crystal are related to the external wave vectors by the apparent depth approximation, i.e.,

$$\mathbf{k}_i=(k_{ix},k_{iy},k_{iz})\simeq(k_{ex},k_{ey},k_{ez}/n) \tag{6}$$

where subscripts e and i refer to external and internal, respectively, and n is the crystal refractive index. Dispersion effects within the crystal will also alter the wave vectors as n is wavelength dependent, however, away from degeneracy when the angle between downconverted photons is larger than 10° the effects of dispersion become small.[11]

The energy conservation δ function can be used to reduce the number of frequency integration variables to one by writing

$$\omega_1=\frac{\omega_0}{2}+\omega,\quad \omega_2=\frac{\omega_0}{2}-\omega\ . \tag{7}$$

Similarly we specialize to directions 1 and 2 close to the symmetric phase-matching directions $\pm\theta$ (measured from the z axis, see Fig. 1) and define

$$\theta_1=\theta+\epsilon_1,\quad \theta_2=-\theta+\epsilon_2\ . \tag{8}$$

This allows us to rewrite the phase-matching integral

$$g_{12}(\Delta t)\propto e^{-i\omega_0(\bar{t}_1+\bar{t}_2)/2}\int d\omega e^{i\omega\Delta t}f(\omega,\epsilon_1,\epsilon_2)\ . \tag{9}$$

The pair-photon spectral amplitude $f(\omega,\epsilon_1,\epsilon_2)$ is obtained by substituting the actual coordinate values of the wave vectors into Eq. (5) noting that phase matching is exact at angles $\pm\theta$ and using small angle approximations for ϵ_1 and ϵ_2.[9] With apertures of limited vertical (y-axis) dimension

$$f(\omega,\epsilon_1,\epsilon_2)=\int d^3r\, h(\mathbf{r})\exp\left[-\frac{ir_x}{c}\left[\omega[2\sin\theta+(\epsilon_1-\epsilon_2)]-\frac{\omega_0}{2}(\epsilon_1+\epsilon_2)\cos\theta\right]\right]$$
$$\times\exp\left[\frac{ir_z}{cn}\left[\frac{\omega_0}{2}\sin\theta(\epsilon_1-\epsilon_2)+\omega\sin\theta(\epsilon_1+\epsilon_2)\right]\right]\ . \tag{10}$$

By combining this equation with Eqs. (9) and (1) we can calculate the coincidence rate $\bar{C}_{12}$. For any finite-thickness crystal the maximum coincidence rate occurs when $\epsilon_1\simeq\epsilon_2$ which is a result of the phase-matching requirements. As a result the term in $r_x\omega(\epsilon_1-\epsilon_2)$ is usually negligible. In the simple theory presented in the following we will also assume a crystal thin enough that the term in $r_z\omega(\epsilon_1+\epsilon_2)$ is negligible being the product of three small variables. This allows analytic results to be obtained. A discussion of corrections arising from this approximation appears in the Appendix.

Substitution of Eq. (9) into Eq. (4) and performing the integral over the long (in terms of optical cycles) coincidence gate time leads to a small aperture coincidence rate of the form

$$\bar{C}(\mathrm{D3,D4})=R^2\bar{C}_{3'4'}+T^2\bar{C}_{34}$$
$$-\beta RT\left[\int f^*(\omega,\epsilon_{3'},\epsilon_{4'})f(-\omega,\epsilon_4,\epsilon_3)\right.$$
$$\left.\times e^{-i2\omega\Delta t}d\omega+\mathrm{c.c.}\right]\ . \tag{11}$$

Here the ω integration limits are assumed to be $\pm\infty$ which is valid in the narrowband approximation.

For point apertures placed *before* the beamsplitter at phase-matched angles $\theta+\epsilon$ and $-\theta+\epsilon$ the difference angles are $\epsilon_3=\epsilon_{3'}=\epsilon_4=\epsilon_{4'}=\epsilon$. Assuming a Gaussian pump beam waist at the crystal with $1/e$ intensity radius σ and combining Eqs. (10) and (11) we obtain

$$\bar{C}(\mathrm{D3,D4})=C_{12}\left[R^2+T^2-2RT\exp\left[-\frac{\sigma^2\omega_0^2\epsilon^2\cos^2\theta}{2c^2}\right]\right.$$
$$\left.\times\exp\left[-\frac{\delta x^2}{2\sigma^2\sin^2\theta}\right]\right] \tag{12}$$

where we define a path-length difference $\delta x=c\Delta t$ and C_{12} is the coincidence rate that would be measured behind the apertures without a beamsplitter. When $\epsilon=0$ there is a Gaussian-shaped coincidence rate reduction around zero path-length difference as expected arising from fourth-order interference. For $R=T=0.5$ the coincidence rate goes to zero when $\delta x=0$. At large δx the coincidence rate is half its value in the absence of a beamsplitter due simply to the random uncorrelated directions chosen by each photon at the beamsplitter. The visibility of the effect decreases rapidly as ϵ increases, moving away from the symmetric phase-matching condition. Thus for high visibility of the effect we require not only phase matching but also overlap of spectra in the two arms of the apparatus. The effect is not, however, confined to a single spatial mode.

In the schematic experiment in Fig. 2(b) where extended detectors D3 and D4 view the crystal through the beamsplitter we can identify transmitted directions 3 and 4 with directions $\theta+\epsilon_4$, $-\theta+\epsilon_3$ and reflected directions 3′ and 4′ with $\theta-\epsilon_3$, $-\theta-\epsilon_4$ where ϵ_3 and ϵ_4 are angles measured from the $\pm\theta$ directions at the detectors. The

total coincidence rate $\bar{C}_{\rm tot}$ is given by an integration over the detector surfaces,

$$\bar{C}_{\rm tot} \propto \int\int d\epsilon_3 d\epsilon_4 \bar{C}(\epsilon_3\epsilon_4) \ . \tag{13}$$

For horizontal slit apertures of angular width Δ centered around the symmetric ($\pm\theta$) directions the integration limits are $\pm\Delta/2$. In the limit $\Delta \ll \theta$ Eqs. (10), (11), and (13) lead to a simple result

$$\bar{C}_{\rm tot} \propto 1 - \frac{2RT}{R^2+T^2} \exp\left[-\frac{\delta x^2}{2\sigma^2 \sin^2\theta} \right] \times \mathrm{sinc}\left[\frac{\omega_0 \Delta \delta x}{2c \tan\theta} \right] . \tag{14}$$

The coincidence reduction as a function of path length changes from a Gaussian with width controlled by the beam-waist radius when slit width Δ is small to a sinc function with width proportional to $1/\Delta$ for wide slits. This is simply the Fourier transform of the pair-photon spectrum which for point apertures is determined primarily by the wave-vector uncertainty at the pump beam waist in the crystal and for wide apertures is a hard-edged top-hat function with width determined by aperture edges. If the apertures are not exactly symmetrical about the $\pm\theta$ directions there will be a loss of visibility similar to that seen in Eq. (12).

Symmetry is also retained when we block the center portions of symmetric slit apertures (see Fig. 3) to create a two-point aperture defining directions $\theta \pm \Delta/2$, $-\theta \pm \Delta/2$. This now ensures overlap between transmitted and reflected spectra and

$$\bar{C}_{\rm tot} \propto 1 - \frac{2RT}{R^2+T^2} \exp\left[-\frac{\delta x^2}{2\sigma^2 \sin^2\theta} \right] \cos\left[\frac{\omega_0 \Delta \delta x}{2c \tan\theta} \right] . \tag{15}$$

The two-point aperture creates a two-peaked spectrum which Fourier transforms to a cosine function within a Gaussian envelope. A similar situation occurs when single-point apertures are placed in front of the detectors *after* the beamsplitter which also ensures spectral overlap. However, in this situation each detector sees only one of the two conjugate wavelengths. It is also clear from Fig. 3 that the two colors overlap at different points on the beamsplitter.

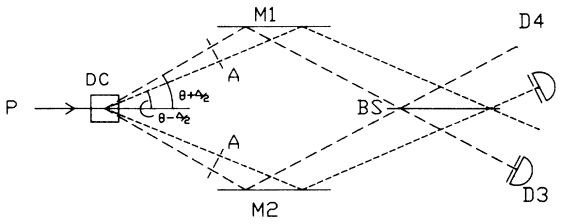

FIG. 3. The apparatus with aperture centers blocked. Abbreviations as in Figs. 1 and 2. Both colors can be viewed by large detectors (shown dotted) although the effects (see Figs. 5 and 6) are similar when each detector only sees one color (shown solid).

III. EXPERIMENT

The schematic of the apparatus is shown in Fig. 2(a). A krypton ion laser with wavelength 413.4 nm illuminates a deuterated potassium dihydrogen phosphate (KD*P) crystal. The crystal is a source of spontaneous parametric fluorescence (or parametric downconversion), which is emitted into a cone around the pump beam. Pair photons were selected from the downconverted light using apertures A placed at points satisfying the phase-matching conditions in the crystal. The photon bandwidth was determined primarily by these apertures, which were horizontal slits of various lengths up to 7.2 mm and height $\sim$1 mm placed 497 mm from the crystal. Light from each arm of the apparatus is combined at a beamsplitter BS and detected in photon-counting detectors D3 and D4. The photon-pair effects are isolated by measuring the coincidence count rate in a multichannel coincidence counter. This effectively allows the photon pairs which are coincident to within a 20-ns gate to be recorded. The path-length difference δX between photon paths 1 and 2 is altered by moving prism $P1$. The coincidence counter is connected to a computer which drives the moving prism, collects the coincidence data, and performs the corrections for accidental coincidences.

Figure 4 shows the result of the experiment performed with 7.2-mm-wide apertures. The smooth curve is the fit to an expression having the form of Eq. (14) with an adjustable visibility parameter V to account for nonideal aperture alignment and beamsplitter tilt. As ω_0 and θ are fixed we can obtain estimates for σ and Δ from the fit parameters: visibility $V=84\%$, pump beam-waist radius $\sigma=94.5\ \mu$m, and aperture angular width $\Delta=11.7$ mrad.

This corresponds to a photon (correlation) length of 39-fs full width at half maximum. Directly measured values of the pump beam waist and aperture width are 78 μm and 14.5 mrad, in approximate agreement with the fitted values. The discrepancy is due to the fact that Eq. (14) assumes that the downconversion crystal has negligible thickness; better agreement is obtained when the 15-

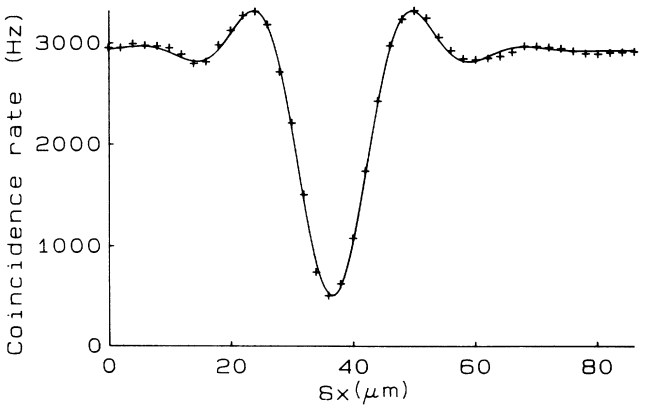

FIG. 4. Coincidence count rate as a function of path-length difference δX for aperture width $A=7.2$, 497 mm from the crystal. The crosses are the experimental coincidence rate, and the curve is the least-squares fit discussed in the text.

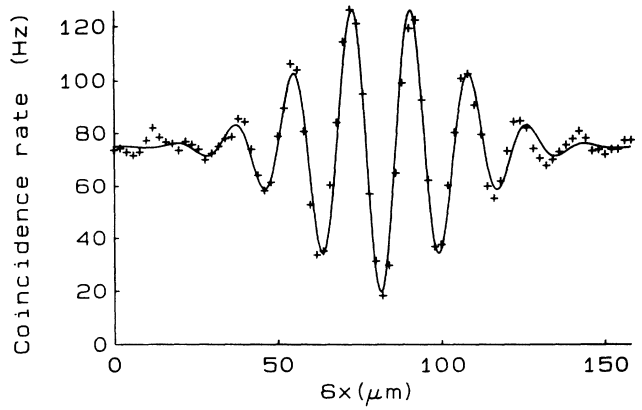

FIG. 5. Coincidence count rate as a function of path-length difference for apertures $A=7.2$ mm with central 5.6 mm blocked (dotted detectors in Fig. 3).

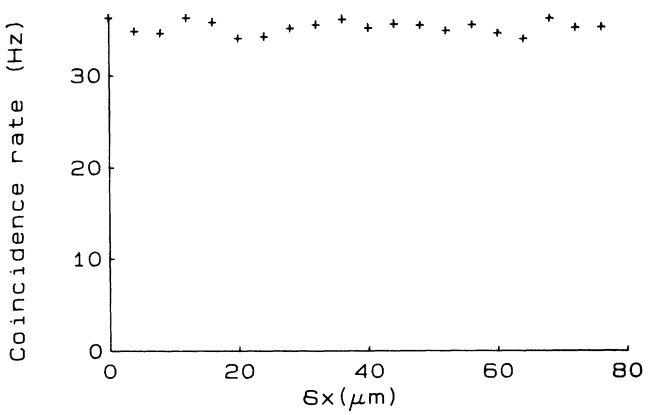

FIG. 7. Coincidence count rate as a function of path-length difference for the same arrangement as Fig. 6, but with one of the four apertures blocked. Shows a loss of the effect as predicted by Eq. (12).

mm length of the crystal is taken into account (see Appendix).

The measured transmission coefficient of the beamsplitter is $T\sim 55\%$ hence we expect a visibility about 98% when alignment is perfect. The 84% visibility seen is due primarily to aperture asymmetry as seen in Eq. (12).

Figure 5 shows the result of the experiment in which the central 5.4 mm of each 7.2-mm-wide aperture was blocked, so that two apertures 0.9 mm wide and separated by 6.3 mm were used in each beam. The smooth curve is the least-squares fit to Eq. (15); as before σ and Δ were left as adjustable parameters. In this case the results of the fits were: visibility $V=74.0\%$, pump beam-waist radius $\sigma=89.0$ μm, and aperture angular width $\Delta=12.1$ mrad.

This corresponds to an oscillation period of 60 fs. The agreement with the actual angular separation of the apertures ($\Delta=12.7$ mrad) is better because the small apertures limit the effective phase-matching depth in the crystal. The estimated beam-waist radius is again high because the theory assumes point apertures whereas they have a finite size (~ 1 mm) in the experiment.

Figure 6 shows the effect of allowing each detector to see only one color which can come from either arm of the apparatus. The effect is largely unchanged apart from a halving of the coincidence rate due to the loss of half the counts at each detector. Figure 7 illustrates the effect of destroying the symmetry before the beamsplitter by blocking one aperture. As predicted by Eq. (12) the effect disappears entirely due to lack of overlap between the pair-photon spectra.

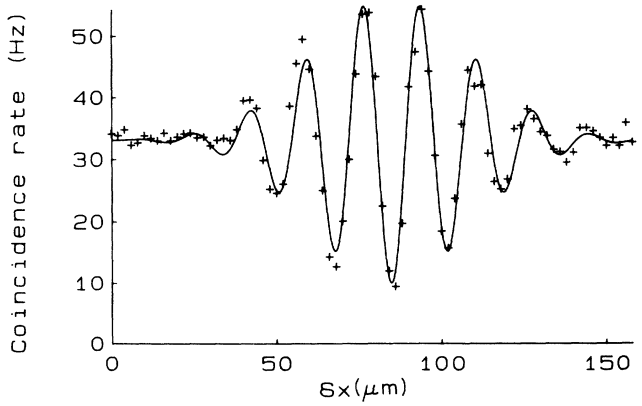

FIG. 6. Coincidence count rate as a function of path-length difference for the same arrangement as Fig. 5, but with the two detectors responding to different wavelengths (solid detectors in Fig. 3).

IV. PROPOSED TEST OF BELL'S INEQUALITY USING TWO-COLOR PHOTONS

Given that the different colors cross at spatially separated points on the beamsplitter we can envisage an apparatus consisting of two beamsplitters as shown in Fig. 8. Apertures are arranged such that color (wavelength) a is recombined at one beamsplitter and its conjugate b recombines at the other. Four detectors labeled by color a,b and position 3,4 view the crystal through the beamsplitter. Coincidence rates between detectors viewing the same color beams will be zero. This leaves four

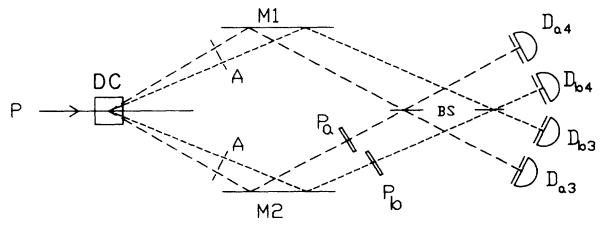

FIG. 8. Proposed arrangement for an experimental test of Bell's inequality. The two colors now recombine at separate beamsplitters. Photons of color a are counted in detectors D_{a4}, D_{a3} and color b in D_{b3} and D_{b4}. The relative phase between the a beams in channels 1 and 2 is adjusted by altering the thickness of phase plate P_a and similarly, for beam b by phase plate P_b.

different possible detector combinations for which coincidences can be measured $\bar{C}(ai,bj)$ with $i=3,4$ and $j=3,4$. Glass plates P_a and P_b are placed in one arm of each color as shown and the resulting gross delay introduced is compensated for by suitable adjustment of the mirror assembly represented by M1. Tilting the plates by small amounts will alter the path length by thicknesses less than the optical wavelength and in this mode the plates act as phase plates. The reduced times and their difference now contain phase delay components p_a, p_b:

$$\bar{t}_{2a}-\bar{t}_{1b}=\Delta t+p_a, \quad \bar{t}_{2a}+\bar{t}_{1b}=2t_1+\Delta t+p_a \tag{16}$$

and similarly with subscripts a interchanged with b. We can now combine the above equations with Eqs. (4), (5), (9), and (10) to obtain an expression for the two-color coincidence rate for point apertures

$$\bar{C}(ai,bj)=R^2\bar{C}_{i'j'}+T^2\bar{C}_{ij}+(-1)^{i+j}\beta RT\left[\int g^*_{ab}(\bar{t}_{i'},\bar{t}_{j'},\tau)g_{ba}(\bar{t}_j,\bar{t}_i,\tau)d\tau+\text{c.c}\right] \tag{17}$$

whence

$$\bar{C}(ai,bj)=R^2\bar{C}_{i'j'}+T^2\bar{C}_{ij}+(-1)^{i+j}\beta RT\left[e^{i\omega_0(p_a-p_b)/2}\int f^*(\omega,\epsilon_{ai'},\epsilon_{bj'})f(-\omega,\epsilon_{ai},\epsilon_{bj})e^{i\omega(p_a+p_b-2\Delta t)}d\omega+\text{c.c}\right]. \tag{18}$$

The prefactor of $(-1)^{i+j}$ arises from the effect of the $\pi/2$ phase change at the beamsplitter which ensures that when the coincidence rate in detectors either side of the beamsplitter is supressed then the rate in detectors on the same side of the beamsplitter are as a consequence increased.[9] The values of the difference angles ϵ are obtained by projection from detectors ai and bj back through the beamsplitter noting that primes indicate reflection at the beamsplitter. Performing the space and frequency integrations assuming point apertures we obtain

$$\frac{\bar{C}(ai,bj)}{\bar{C}_R}=1+(-1)^{i+j}V\exp\left[-\frac{\delta x'^2}{2\sigma^2\sin^2\theta}\right]\times\cos\left[\Phi_a+\Phi_b+\frac{\omega_0\Delta\delta x}{2c\tan\theta}\right] \tag{19}$$

with $\Phi_a=\omega_a p_a$ and $\Phi_b=\omega_b p_b$. Frequencies of colors a and b are given by

$$\omega_{a/b}=\omega_0\left[1\pm\frac{\Delta}{\tan\theta}\right]/2, \tag{20}$$

modified displacement by

$$\delta x'=c(\Delta t-p_a-p_b), \tag{21}$$

and visibility

$$V=V'\frac{2RT}{R^2+T^2} \tag{22}$$

where V' accounts for reduction of visibility from misalignment. This result differs from Eq. (15) in that the extra phase factors can change the phase of the cosinusoidal oscillation with respect to the Gaussian envelope. When the movable mirror is adjusted such that $\delta x\simeq 0$ the coincidence rate can be varied simply by tilting the phase plates P_a and P_b to alter their thicknesses by fractions of a wavelength. With $\delta x=0$ and phase plate differences $cp_{a,b}\ll\sigma\sin\theta$ then

$$\frac{\bar{C}(ai,bj)}{\bar{C}_R}=1+(-1)^{i+j}V\cos(\Phi_a-\Phi_b). \tag{23}$$

This is formally equivalent to the polarization correlation for a pair of photons in an s state[12,13] (although conventionally it is written as a phase difference). A maximum coincidence rate at detectors ai,bj is obtained by tuning the phase delays to ensure the argument of the cosine term in Eq. (23) is π. This also implies a maximum coincidence rate between the other two detectors aj,bi. More significantly, one can redistribute the coincidences in detector pairs $a3,b4$ and $a3,b3$, by adjusting the phase plate P_a, apparently remotely altering the direction that the *coincident* b-color photons take at the beamsplitter. Hence this effect can be used as a demonstration of quantum-mechanical violations of local realistic theories.

To formulate a Bell[13,14] inequality in this system we define the normalized quantity

$$P(\Phi_a,\Phi_b)=\frac{\bar{C}(a3,b4)+\bar{C}(a4,b3)-\bar{C}(a4,b4)-\bar{C}(a3,b3)}{\sum_{ai,bj}\bar{C}(ai,bj)} \tag{24}$$

where the normalizing constant is an estimate of the total number of coincidences in all detector pairs. Choosing four phase angles $\Phi_a=0$, $\Phi_b=\pi/4$, $\Phi'_a=\pi/2$, $\Phi'_b=3\pi/4$ we can formulate the normal Bell inequality test by measuring the quantity

$$P(\Phi_a,\Phi_b)-P(\Phi_a,\Phi'_b)+P(\Phi'_a,\Phi_b)+P(\Phi'_a,\Phi'_b)=2\sqrt{2}V. \tag{25}$$

A local analysis[13,14] would lead to a result no greater than two hence we can in principle demonstrate a violation of the Bell inequality when $V>0.71$. Returning to the experimental section we see that the visibility of the two-aperture effect (Fig. 5) is 0.74 hence a suitable rearrangement of the apparatus to the form shown in Fig. 8 will allow such a measurement. Bell inequality experiments based on the superposition of orthogonally polarized photons at a beamsplitter have already been demonstrated,[12,15] however, the authors know of no experimental tests of local realism based on phase and momentum proposed here. This experimental arrangement is, however, similar to one proposed[16] during the preparation of this

manuscript and is closely related to other recently published polarization-independent tests of the Bell inequality.[17–19]

V. DISCUSSION

We have demonstrated a fourth-order interference effect between multimode photons. The effect arises when broadband pair photons are recombined at a beamsplitter and is characterized by a large reduction in the coincidence rate measured between photon-counting detectors placed beyond the beamsplitter. Using symmetrically phase-matched horizontal slit apertures as the sole limit of photon bandwidth a 39-fs (FWHM) photon "cross-correlation" length has been measured with shape reflecting the Fourier transform of the pair-photon bandwidth. We believe this to be the shortest effect measured to date. To achieve a shorter photon length will require a thinner crystal but in principle photons of a few optical cycles could be measured. For photons of relative bandwidth greater than 10% the narrowband approximation used here breaks down and a full nonanalytic theory is required.[20]

We have also demonstrated a fourth-order spatial beating effect by recombining pair photons containing two distinct frequencies at the beamsplitter. The oscillating coincidence rate measured reflects the frequency difference between the two colors. The geometry is such that the different frequencies overlap at different locations on the beamsplitter. By introducing phase delays in one arm of each color the phase of the oscillation can be changed. With suitable choice of phase delays violations of local realistic theories can be demonstrated.[21] Some arguments against the Bell inequality arise because the effective quantum efficiencies in the coincidence channels have in the past been extremely low. In this sort of apparatus we are already achieving net efficiencies of up to 15% (Ref. 22) with present solid-state photon-counting detectors. Theoretically achievable device efficiencies are above 80%, which may allow definitive measurements to be made.

Because of the high net efficiencies the count rates can be high. Here the wide aperture effect shows a count rate change of some 2.5 kHz. With this sort of count rate we can begin to think of ways of exploiting the effect to probe two photon interactions with materials. Furthermore, the effect of placing dispersive media in the beam paths could produce some interesting effects.

ACKNOWLEDGMENTS

The authors are grateful to Professor R. Loudon and Professor E. Jakeman for their encouragement and useful discussion on this work.

APPENDIX

To calculate the effect of finite crystal thickness on our results we substitute the full form of Eq. (10) into Eq. (11) and integrate over the finite horizontal slit apertures as indicated in Eq. (14). Transforming to sum and difference variables and rearranging the integration order to perform the ω integration first we obtain

$$\frac{\bar{C}_{\rm tot}}{\bar{C}_R}=1-\frac{2RT}{R^2+T^2}\times\frac{\int_A d\epsilon_s d\epsilon_d \int d\mathbf{r}_s d\mathbf{r}_d h(\mathbf{r}_s)h(\mathbf{r}_d)\exp[(i\omega_0/2nc)(r_{xs}n\epsilon_s\cos\theta-r_{zs}\epsilon_d\sin\theta)]\delta(2r_{xs}\sin\theta-r_{zd}(\sin\theta)\epsilon_s/n-2c\Delta t)}{\int_A d\epsilon_s d\epsilon_d \int d\mathbf{r}_s d\mathbf{r}_d h(\mathbf{r}_s)h(\mathbf{r}_d)\exp[(i\omega_0/2nc)(r_{xd}n\epsilon_s\cos\theta-r_{zd}\epsilon_d\sin\theta)]\delta(2r_{xs}-r_{zd}\epsilon_s/n)} \tag{A1}$$

where sum and difference coordinates are defined as

$$\begin{aligned}&\epsilon_s=\epsilon_3+\epsilon_4,\quad \epsilon_d=\epsilon_3-\epsilon_4\ ,\\ &r_{xs}=r_{x1}+r_{x2},\quad r_{xd}=r_{x1}-r_{x2}\ ,\\ &r_{zs}=r_{z1}+r_{z2},\quad r_{zd}=r_{z1}-r_{z2}\ ,\end{aligned} \tag{A2}$$

$\delta(X)$ is the Dirac δ function, C_R the random overlap coincidence rate at large path-length differences, and a narrow beam waist is assumed (terms in $r_d\epsilon_d$ small). A more transparent version of this equation can be obtained by writing

$$2c\Delta t+r_{zd}(\sin\theta)\epsilon_s/2n=2c\Delta t'=2\Delta x'\ . \tag{A3}$$

Given that the upper and lower integrations in Eq. (A1) are equal when $\Delta t=0$ and assuming a Gaussian beam of $1/e$ intensity width σ such that $h(r_{xs})=\exp(-r_{xs}^2/2\sigma^2)$ and a crystal length L then Eq. (A1) simplifies to

$$\frac{C_{\rm tot}}{C_R}=1-\frac{V}{N}\int_{-\Delta}^{\Delta}d\epsilon_s\int_{-L}^{L}dr_{zd}\exp\left[-\frac{\delta x'^2}{2\sigma^2\sin^2\theta}\right]\times\exp\left[i\frac{\omega_0\delta x'\epsilon_s}{2c\tan\theta}\right] \tag{A4}$$

which is clearly equivalent to Eq. (14) when the crystal is thin and $\delta x\simeq\delta x'$. The normalizing constant N is obtained from the lower integral of Eq. (A1) in a similar way and $V=2RT/(R^2+T^2)$. Equation (A4) is nonanalytic but can be integrated digitally. Performing the integration on a computer we obtain a sinc-like coincidence reduction with full width at half maximum 39 fs agreeing well with the data when parameter values are as given in the experimental section ($\Delta=14.5$ mrad, $\theta=14.8°$, $\sigma=78$

μm, and $2\pi c/\omega_0 = 0.413$ μm) and effective crystal length is limited to $L = 6.8$ mm. This limited effective crystal depth (true length is 15 mm) is primarily due to the fact that the apertures are placed a finite distance from the crystal and projected beam dimension in the crystal is comparable with the aperture dimension. The theory to date takes the paraxial approximation which ignores these effects.

[1]D. C. Burnham and D. L. Weinberg, Phys. Rev. Lett. **25**, 84 (1973).

[2]B. R. Mollow, Phys. Rev. A **8**, 2684 (1973).

[3]H. Fearn and R. Loudon, Opt. Commun. **64**, 485 (1987).

[4]Z. Y. Ou, C. K. Hong, and L. Mandel, Opt. Commun. **63**, 118 (1987).

[5]Z. Y. Ou, Phys. Rev. A **37**, 1607 (1988).

[6]H. Fearn and R. Loudon, J. Opt. Soc. Am. B **6**, 917 (1989).

[7]R. A. Campos, B. E. A. Saleh, and M. C. Teich, Phys. Rev. A **40**, 1371 (1989).

[8]C. K. Hong, Z. Y. Ou, and L. Mandel, Phys. Rev. Lett. **59**, 2044 (1987).

[9]J. G. Rarity and P. R. Tapster, in *Photons and Quantum Fluctuations,* edited by E. R. Pike and H. Walther (Hilger, London, 1988), p. 122; see also J. Opt. Soc. Am. B **6**, 1221 (1989).

[10]Z. Y. Ou and L. Mandel, Phys. Rev. Lett. **61**, 54 (1988).

[11]See, for example, C. K. Hong, Ph.D. thesis, University of Rochester, 1988, p. 26.

[12]Z. Y. Ou and L. Mandel, Phys. Rev. Lett. **61**, 50 (1988).

[13]J. F. Clauser and A. Shimony, Rep. Prog. Phys. **41**, 1881 (1978).

[14]J. S. Bell, in *Foundations of Quantum Mechanics,* edited by B. d'Espagnat (Academic, New York, 1971), pp. 171–181.

[15]Y. H. Shih and C. O. Alley, Phys. Rev. Lett. **61**, 2921 (1988).

[16]M. A. Horne, A. Shimony, and A. Zeilinger, Phys. Rev. Lett. **62**, 2209 (1989).

[17]M. D. Reid and D. F. Walls, Phys. Rev. A **34**, 1260 (1986).

[18]P. Grangier, M. J. Potasek, and B. Yurke, Phys. Rev. A **38**, 3132 (1988).

[19]J. D. Franson, Phys. Rev. Lett. **62**, 2205 (1989).

[20]S. Sarkar and E. R. Pike, Europhys. Lett. **7**, 581 (1988).

[21]J. G. Rarity and P. R. Tapster (unpublished).

[22]J. G. Rarity, K. D. Ridley, and P. R. Tapster, Appl. Opt. **26**, 4616 (1987).